

Quadruped Trotting with Passive Knees - Design, Control, and Experiments

Geoff Hawker and Martin Buehler¹

Center for Intelligent Machines, Ambulatory Robotics Laboratory

McGill University, Montreal, QC, H3A 2A7 Canada, <http://www.cim.mcgill.ca/~arlweb>

Abstract

A locking, unactuated knee is added to the Scout II quadruped robot and trotting gaits are studied. The mechanical design of the knee is presented, trotting algorithms are discussed, and a control approach for a robotic leg with an unactuated knee is developed. A model of a single leg is used to determine appropriate leg trajectory parameters and initial conditions to achieve trots. The single leg system and the complete robot are simulated. Experimental implementation of single leg control and quadruped trotting on Scout II are presented.

1 Introduction

The field of mobile robotics has reached a maturity that has resulted in an increased number of applications. Some current uses include surveillance of hazardous or dangerous environments such as volcanoes or chemical accident sites, delivery tasks in hospitals or factories, minefield clearance, or bomb disposal. The majority of these devices are wheeled or tracked. Their inherent static stability has made them an attractive first step for practical applications. However, wheels and tracks have limitations when it comes to negotiating uneven terrain or climbing stairs. Biology has shown that legs are an excellent means of traversing varied environments. Consequently, many researchers, including the members of the Ambulatory Robotics Laboratory (ARL), have been investigating legged robotic locomotion.



Figure 1 - Trot diagram from Working Model simulation .

Earlier work at ARL showed that simple quadruped robots, with only one degree of freedom (DOF) per leg are capable of walking, turning, and step-climbing using primarily a bound-type of motion [4][5]. Following the same philosophy of developing quadrupedal robots of limited complexity, the current research investigates quadrupedal trotting with unactuated knees. Each leg has an actuated hip joint and an unactuated knee joint with a locking mechanism. Scout II is now able to trot, a gait where diagonal legs are used in pairs. One pair operates as the support legs while the others swing forward. This general type of trot gait is shown in Figure 1. McGeer showed that it is possible for a planar biped with knees to

walk down an incline powered only by gravity [8]. Of interest as well is past work on underactuated manipulators. Arai and Tachi showed how position control of a 2 DOF manipulator with one actuator and one brake on the passive joint can be achieved [1][2]. They used a two part method in which point-to-point control is achieved using dynamic coupling between the active and passive joints. Bergerman et al. [6][7] developed an index which quantifies the dynamic coupling of an underactuated system and they verified it experimentally with a two-link underactuated manipulator.

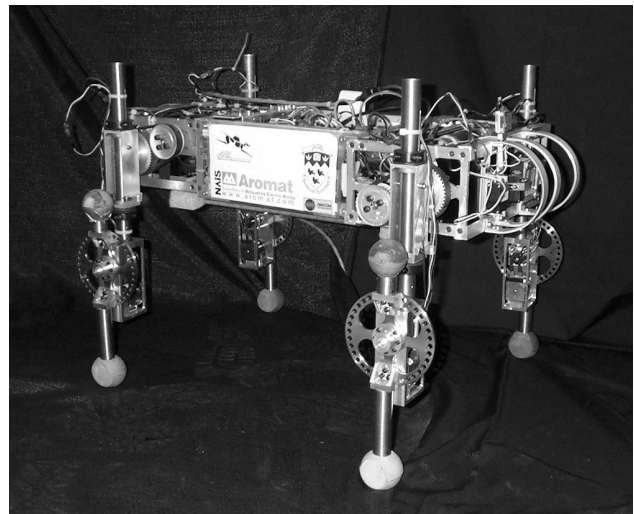


Figure 2 - Scout II with unactuated knees

2 Mechanical Design and Experimental Setup

The experimental work is based on the Scout II quadruped developed at ARL [3]. Prior to this research, bounding and pronking gaits were investigated with Scout II having an additional spring-loaded, unactuated prismatic joint in each leg. For this work, the prismatic joint was replaced with an unactuated revolute knee joint (Figure 2 and Figure 3). Optical encoders measure the hip angles and potentiometers the knee angles.

Scout II is 90 cm long, 58 cm wide, and has a total height above the ground (when the legs point straight down) of 54 cm. It weighs roughly 30 kg. Since the controllers are

¹ This project was supported in part by IRIS, a Federal Network of Centers of Excellence, and the National Science and Engineering Research Council of Canada (NSERC).

developed in the saggital plane, the robot was mounted on a treadmill using a "Planarizer" - a device of linear and rotational bearings to keep its motion planar for the majority of the experimental work. The unactuated knees can be locked and unlocked every 10° by an electrically efficient latching solenoid, thereby reducing the power consumption and weight as compared to traditional brakes, an important consideration for mobile robotics.

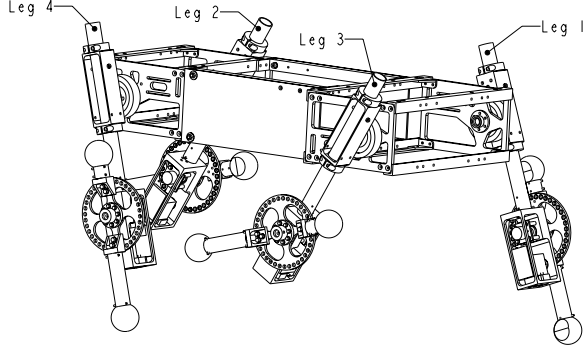


Figure 3 - Scout II trotting with passive knees

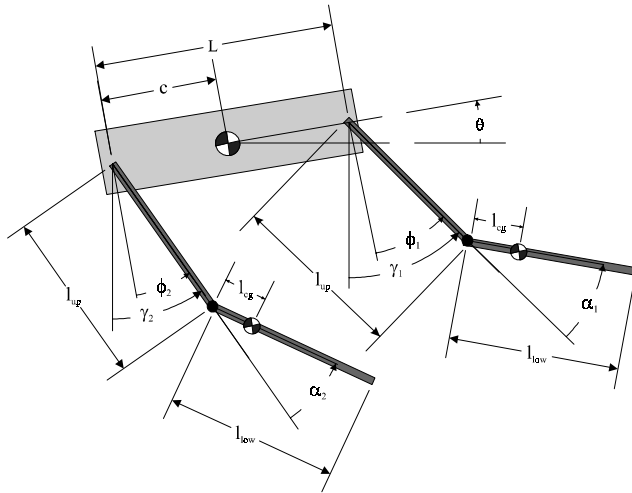


Figure 4 - Planar model of Scout II (legs 3 and 4 omitted)

3 Trotting Algorithms

Two types of trot are analyzed: the step-trot, and the controlled velocity trot. In the step-trot, the robot has zero forward velocity at the start and the end of each step. The controlled-velocity trot permits the control of the robot's forward velocity, which includes maintaining a constant speed, and ramping the speed up or down. In both cases, the general algorithm is to use legs 1 and 4 operating as a pair, and legs 2 and 3 doing the same (Figure 1 and Figure 3). One of the pairs is the support pair, while the other pair is the free pair and unlocks their knees to control the knee angle trajectories using the dynamic coupling with the upper leg. The knees are controlled to achieve toe clearance while the free legs swing forward. Once the free legs are straight, they are brought to the desired touchdown angle. The cycle then

repeats with the leg pairs switching roles as the support and the free pairs.

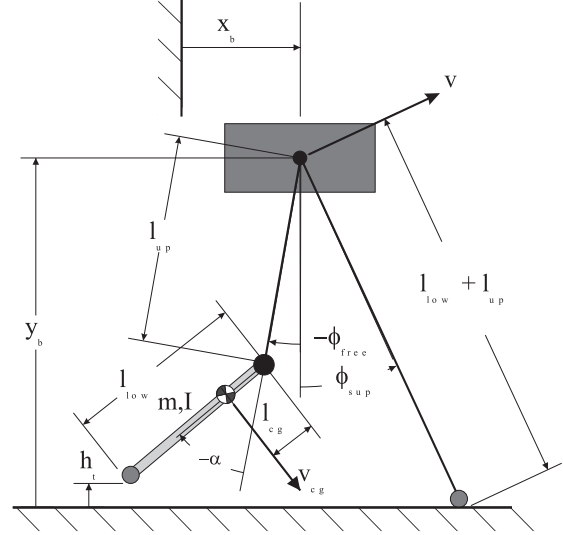


Figure 5 - Single Leg Model

The trot is divided into states, which are defined as follows. In state 11, legs 2 and 3 are support legs. They sweep towards the rear of the robot propelling it forward. Knees 1 and 4 are unlocked, and upper legs 1 and 4 sweep towards the front of the robot while deflecting their knees back to achieve toe clearance. Legs 2 and 3 continue to sweep towards the rear of the robot in state 12. Once knees 1 and 4 have reached 0° , they are locked and the now locked free legs are controlled to the desired touchdown angle. States 21 and 22 are the same as states 11 and 12 respectively, but with leg pairs 1-4 and 2-3 switched. Figure 3 shows the robot in state 21. In both types of trots, the knee angle is controlled to follow a sinusoidal trajectory where the initial and final angle is 0° , and there is no initial or final angular velocity. The cycle time ($T_{LS\alpha}$) and the magnitude of the maximum deflection (α_{amp}) are parameters that were selected by using the simulations. Figure 4 shows the planar model of Scout II with legs 3 and 4 omitted for clarity, and Table 1 lists the nomenclature.

L	Total body length
C	Distance of center of mass from rear of robot
l_{up}	Length of upper leg
l_{low}	Length of lower leg
l_{cg}	Distance of center of mass of lower leg from the knee
θ	Body pitch
$\phi_{1,2,3,4}$	Upper leg angle with respect to the body
$\gamma_{1,2,3,4}$	Upper leg angle with respect to the vertical
$\alpha_{1,2,3,4}$	Knee angle - angle of lower leg with respect to upper leg

Table 1 - Scout II planar model nomenclature

The support leg trajectory for the step-trot is

$$\phi_{sup}(t) = \frac{(\phi_0 + \phi_f)}{2} + \frac{(\phi_0 - \phi_f)}{2} \cos\left(\frac{\pi}{t_f} t\right) \quad (1)$$

where ϕ_0 and ϕ_f are the initial and final angles respectively, and t_f is the cycle time. The support leg trajectory for the controlled velocity trot is

$$\phi_{\text{sup}}(t) = \sin^{-1} \left(\sin \phi_0 - \frac{v \cdot t}{l_{\text{low}} + l_{\text{up}}} \right) \quad (2)$$

4 Single Leg Model

In order for the robot to trot successfully, it is imperative that the toes clear the ground while the free legs swing forward, and that the knee is locked at a ϕ angle that is greater than the desired touchdown angle. However, in the passive knee system, both the ϕ and the α angles of a single leg cannot be controlled at the same time. The approach used here is to control the knee angle first, to lock it, and then to use ϕ control to bring the knee to the desired touchdown angle. By developing a single leg model and iterating through solutions based on this desired knee angle trajectory, proper trajectory parameters and initial conditions can be selected such that the initial knee angle control also brings the ϕ angle close to the desired touchdown angle at the time of knee lock. Then, the ϕ angle can be "fine-tuned" during states 12 or 22 (depending on which leg-pair is free) to bring it to the desired touchdown angle. In this section, the equation of motion (EOM) of a single leg system is presented, the approach to solving it for different trajectory parameters and initial conditions is discussed, and the results are tabulated.

Figure 5 shows the single leg model, and Table 2 lists the nomenclature used. Through previous work at ARL, it is known that near perfect tracking of the support and free leg angles (ϕ_{sup} and ϕ_{free}) can be achieved via PD control, which implies that the upper leg can be considered to be massless, and the support leg angle can be taken as a position input to the system. It can be seen that this system only has one degree of freedom, α , and no torque inputs. We also assumed that the knee joint is frictionless, and that the ϕ angle can be considered to be with respect to the vertical as well as with respect to the body. This assumption is valid if there is no pitching of the body, which is true for trotting gaits. The equation of motion was developed using the Lagrangian technique and can be written as:

$$\begin{aligned} \ddot{x}_b \cos(\phi_{\text{free}} + \alpha) + \ddot{y}_b \sin(\phi_{\text{free}} + \alpha) + l_{\text{up}} \ddot{\phi}_{\text{free}} \cos \alpha - l_{\text{up}} \dot{\phi}_{\text{free}} \dot{\alpha} \sin \alpha \\ + l_{\text{cg}} (\ddot{\phi}_{\text{free}} + \ddot{\alpha}) + \frac{I}{m l_{\text{cg}}} (\ddot{\phi}_{\text{free}} + \ddot{\alpha}) + l_{\text{up}} \dot{\phi}_{\text{free}} (\dot{\phi}_{\text{free}} + \dot{\alpha}) \sin \alpha \\ + g \sin(\phi_{\text{free}} + \alpha) = 0 \end{aligned} \quad (3)$$

It is assumed that the α tracking can also be considered as near perfect (this is verified in the next section of this paper). Therefore, in addition to the support leg trajectory (for either the step-trot or the controlled velocity trot of section 3), the desired α trajectory can be considered as an input into the EOM and the system can be solved for ϕ_{free} as a function of the ϕ_{sup} and α trajectories. $x_b(t)$ and

$y_b(t)$ are calculated geometrically based upon the support leg ϕ trajectory. This was done for both the step trot and the controlled velocity trot while iterating through the following trajectory parameters and initial conditions:

- initial ϕ_{free} varying from -10° to -40° , every 10°
- α_{amp} varying from -5° to -30° , every 5°
- $l_{\text{up}} = 0.20$ and 0.10 m
- $T_{\text{LS}} = 1$ second, $T_{\text{LS}\alpha} = 0.75$ seconds
- robot velocity 0.1 to 0.8 m/s every 0.1 m/s (controlled velocity trot only)

As an example, the plots of the results for the step-trot with $l_{\text{up}} = 0.20$ m are included as Figure 6. In the simulation, ground contact for the swing leg was neglected, and consequently, toe heights that are equal to or less than 0.0 m represent the toe dragging on the ground. It can be seen from the plots that for all trajectory parameters studied, there is significant toe drag, but it is minimized for an initial ϕ_{free} of -10° . Furthermore, it can be seen that the toe height is maximized for increasing α_{amp} , but that this comes at the expense of a larger error between the ϕ angle at knee lock and the desired ϕ angle at touchdown. Therefore, an α_{amp} of -30° was the best selection.

x_b	horizontal position of hip
y_b	vertical position of hip
l_{up}	upper leg length
l_{low}	lower leg length
l_{cg}	distance of center of mass of lower leg from knee joint
ϕ_{free}	swing leg angle with respect to the vertical
ϕ_{sup}	support leg angle with respect to the vertical
α	knee angle with respect to upper leg
m	mass of lower leg
I	moment of inertia of lower leg about center of mass
h_t	height of toe from ground
v_{cg}	velocity of center of mass of lower swing leg
v	velocity of hip

Table 2 - Single leg model nomenclature

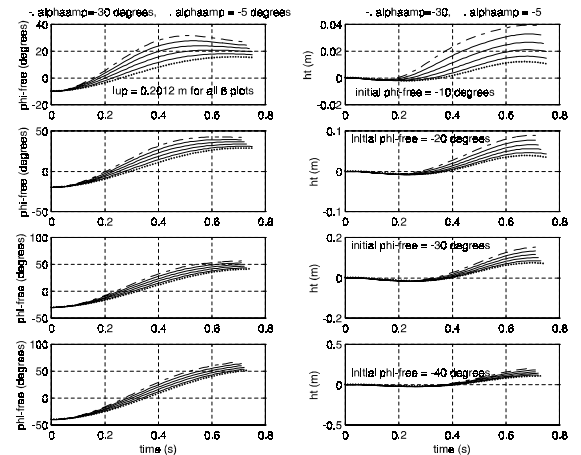


Figure 6 - ϕ_{free} and toe-height of swing leg for step-trot with $l_{\text{up}} = 0.20$ m

A similar analysis was done for the shorter leg configuration step trot and the controlled velocity trot. From these studies, the best sets of parameters were determined for achieving the two types of trots, where the criteria are to minimize toe drag, to maximize toe height throughout the cycle, and to minimize the error between ϕ at knee lock and the desired ϕ touchdown angle. These results are tabulated in Table 3 and Table 4. The system showed a negative toe height throughout the cycle for all velocities above 0.8 m/s, which implies a 0.7 m/s limit for this robot. Although the constant velocity plots are not shown, another observation is that there was never any toe drag at any velocities for the controlled velocity trot.

α_{amp}	-30°
l_{up}	0.20 m
Initial ϕ_{free}	-10°
Initial ϕ_{sup}	10°
T_{LS}	1 s
$T_{LS\alpha}$	0.75 s

Table 3 - Optimized parameters for step-trot

velocity	initial ϕ_{free}	α_{amp}	l_{up}	T_{LS}	$T_{LS\alpha}$
0.1 m/s	-10°	-30°	0.20 m	1.0 s	0.75 s
0.2 m/s	-10°	-30°	0.20 m	1.0 s	0.75 s
0.3 m/s	-20°	-30°	0.20 m	1.0 s	0.75 s
0.4 m/s	-20°	-30°	0.20 m	1.0 s	0.75 s
0.5 m/s	-30°	-30°	0.20 m	1.0 s	0.75 s
0.6 m/s	-30°	-30°	0.20 m	1.0 s	0.75 s
0.7 m/s	-40°	-30°	0.20 m	1.0 s	0.75 s

Table 4 - Optimized parameters for a controlled velocity trot

5 Single Leg Control - Simulation and Experiment

Control of the knee angle is performed by using the knee angle position as the feedback term for the torque control of the hip actuator. A PID controller as shown in (4) was used. The dynamic coupling between the upper leg and the lower leg (the hip and the knee) is such that a positive torque in the hip actuator will cause a negative torque in the knee. Consequently, (4) is simply the negative of the standard PID controller where the actuator is directly coupled to the joint. In (4), t_{start} is the start time of the state.

$$\tau = -K_{p\alpha}(\alpha_d - \alpha) - K_{d\alpha}(\dot{\alpha}_d - \dot{\alpha}) - K_{i\alpha} \int_{t_{start}}^t (\alpha_d - \alpha) dt \quad (4)$$

To verify the validity of the trot approach of section 3, the single leg system was simulated in Working ModelTM and the same experiment was performed on one leg of the robot while the robot was locked in place above the ground on a stand. The details of the simulation are discussed in section 6. For both cases, leg 1 was cycled throughout states 11, 12, 21, and 22 as it would be when

the robot is actually trotting on the ground. The step trot algorithm was implemented with the parameters from Table 3. The controller gains for each state were chosen experimentally. Furthermore, a motor model was implemented in the simulation to limit the torques commanded from the controller to those that can actually be achieved, or that in the case of motor saturation, the desired behavior could still be maintained. These motor-torque limits were those provided by the manufacturer.

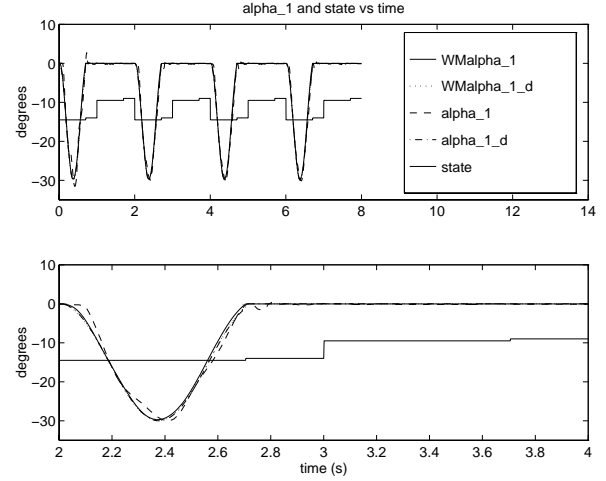


Figure 7 - α actual and desired and scaled state vs. time for single leg experiment on Scout II and for the same experiment simulated in Working ModelTM. The second graph is a closer view of 2 seconds of the same data

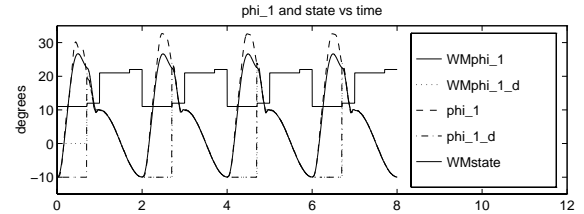


Figure 8 - ϕ actual and desired and state vs time for single leg experiment on Scout II and for the same experiment simulated in Working ModelTM

Figure 7 shows the α trajectory of leg 1 (desired and obtained) as it is cycled through all the trot states for the simulation and for the actual experiment. It can be seen that in the simulation, near perfect tracking is obtained, and in the actual experiment, very good tracking is achieved with minimal errors. The largest error is at the beginning and the end of the cosine trajectory while the solenoid is unlocking or locking the knee causing some small delays. The horizontal lines show the states.

Figure 8 shows the plot of ϕ_1 (desired and obtained) vs time for both the simulation and the actual experiment. It can be seen that during state 11, when knee 1 is unlocked and the knee angle is being controlled using the hip actuator and the controller of (4), that the hip angle (ϕ) reaches a larger value near the end of the state. The dynamic coupling is larger in the simulation because friction was neglected. In the actual robot, despite having

teflon coated bearings for the knee joint, some friction still remained which forced the hip motion to be a bit more dramatic to achieve the same knee angle trajectory. Nevertheless, the ϕ angle at knee lock is very similar in both cases, and the support sweep during states 21 and 22 agree very closely between the desired and the actual values for both the simulation and the actual system. Please note that during state 11, the ϕ angle is not controlled to follow a desired ϕ trajectory, which is why the desired trajectory curves are kept flat.

6 Trotting Simulations

The simulation package used for this research is Working Model™, made by Knowledge Revolution. This is a graphical, dynamic mechanical system simulator in which models are constructed as rigid bodies, constraints, and inputs. The software integrates the system at a user-specified time step. The quadruped system was modeled using the mass, inertia, and geometric properties of the actual Scout II robot. In addition, the motor model was implemented, and the time step was chosen to be the same as the experimentally determined time step of 1.5 ms in the actual system. Both the step-trot and the controlled velocity trot were simulated.

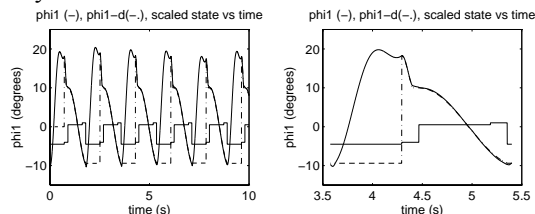


Figure 9 - ϕ_1 actual and desired, and scaled state vs. time for step-trot

The **step-trot** algorithm was implemented in simulation using the parameters and initial conditions of Table 3. Figure 9 shows ϕ_1 for a 10 s step-trot along with a closer view of some of the data. It can be seen that the behavior is very repeatable. Although the data is not included, the knee angle tracking (α) was the same as in Figure 7. Figure 10 shows the height of toe 1 for the same 10 s trot. The close-up view shows a short toe drag period at the start of state 11, which was predicted in the mathematical analysis of section 4. Although the plots are not presented, the remaining three legs exhibited very similar behaviors.

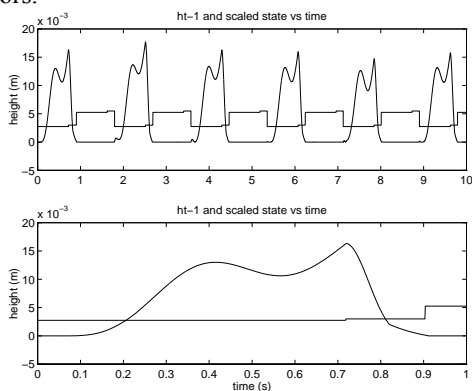


Figure 10 - toe height 1, scaled state vs. time for step-trot

The **controlled velocity trot** was implemented in simulation for a desired velocity profile of a ramp up and down to 0.4 m/s using the velocity dependent parameters of Table 4. Figure 11 shows the velocity response of the system, where the dashed line represents the desired velocity. It can be seen that the overall velocity tracking is quite good, but as the velocity increases, the actuators become saturated and there is a loss of velocity at touchdown. However, the controller is robust enough to return to the desired velocity prior to the next touchdown.

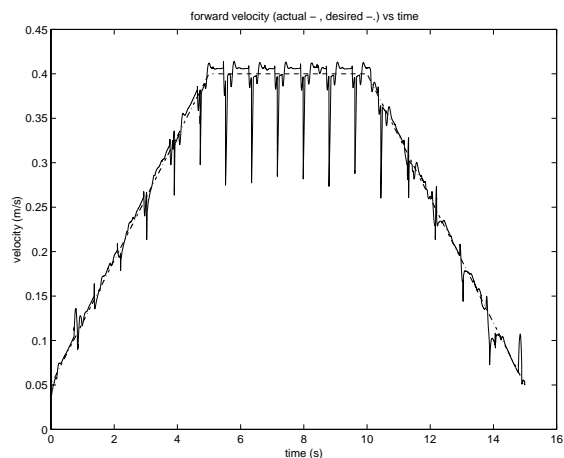


Figure 11 - Controlled velocity trot ramp up and down

7 Trotting Experimental Results

The Scout II robot was mounted onto a treadmill using the planarizer, which limits the robot's motion to the saggittal plane. This eliminated the need for active control of body roll about the diagonal axes during trotting, which is the subject of future research.

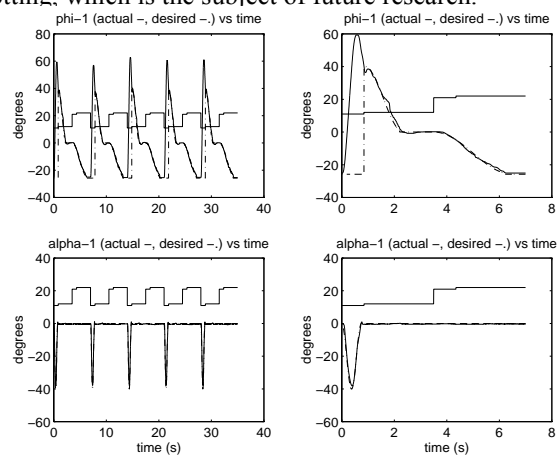


Figure 12 - ϕ_1 and α_1 (desired and actual) and scaled state vs time for step-trot (experimental data)

Experimental trotting of the Scout II robot on the treadmill was successful. Figure 12 shows the ϕ_1 and α_1 trajectories for a 35 s step-trot. The experiment was stopped by the researcher, and not because the robot

stumbled. It can be seen that the shape of the ϕ trajectory during control (state 11) is similar to the simulated results (Figure 9) and that the support ϕ trajectories (states 21 and 22) track the desired values quite well.

Figure 13 shows the toe height of leg 1 for the same step-trot. The second plot shows the toe height for states 11 and 12 for the first cycle. It can be seen that the toe height is positive for all of state 11 and that it touches the ground during state 12 at the desired touchdown angle.

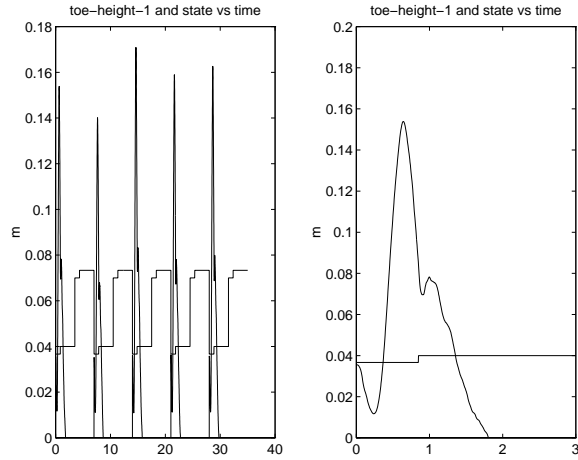


Figure 13 - toe height of leg 1 and scaled state vs. time for step-trot (experimental data)

Although a successful step-trot was achieved, the experimental parameters and initial conditions that were used to obtain a stable step-trot on the treadmill (Table 5) are significantly different from the simulation values (Table 3). However, it is important to note that the general trajectory shapes are the same, and that the resulting trot is stable. The discrepancies are due to unmodeled factors. For example, the solenoids selected were not strong enough to unlock the knee when the leg was bearing any weight. To accommodate this, the initial free leg angle was selected to be greater in magnitude (though opposite in sign) of the touchdown angle (initial support angle). Consequently, the toe was in the air at the time of unlocking, and the symmetry of the initial free leg and support leg angles was lost. The second plot of Figure 13 shows that at the start of the cycle (state 11), the toe height was not zero, but close to 4.0 cm.

α_{amp}	40.1°
initial ϕ_{free}	25.8°
initial ϕ_{sup}	0.0°
T_{LS}	3 s
$T_{LS\alpha}$	0.75 s
wait between cycles	0.5 s

Table 5 - Trajectory parameters and initial conditions for experimental step-trot

An additional source of discrepancy is that the upper legs of the robot are actuated through a belt transmission, which has a backlash of several degrees; the encoder is on the motor shaft, and therefore the measured support leg angle can have an error of equivalent magnitude. To compensate for this, the initial support leg angle had to be

reduced significantly, and the total cycle (T_{LS}) had to be increased to give the free legs time to clear the ground. Furthermore, the amplitude of the knee trajectory had to be increased to ensure ground clearance.

We are encouraged by the successful implementation of the step-trot, and are in the process of implementing the controlled velocity trot.

8 Conclusion

A passive knee system was added to the existing Scout II quadruped. A control approach of the passive knee system for step and controlled velocity trotting was presented. A single leg model was developed and used to determine appropriate trajectory parameters and initial conditions. These conditions were verified in simulation. Despite differences between the actual and simulated response, a stable trot was achieved in experiment.

References

- [1] H. Arai, S. Tachi. Position Control of a Manipulator with Passive Joints Using Dynamic Coupling. In *IEEE Transactions on Robotics and Automation*, pages 528-534, August 1991.
- [2] H. Arai, S. Tachi. Position Control System of a Two Degree of Freedom Manipulator with a Passive Joint. In *IEEE Transactions on Industrial Electronics*, pages 15-20, February 1991.
- [3] R. Battaglia. Design of the SCOUT II Quadruped with Preliminary Stair-Climbing. Master's Thesis, McGill University, Montreal, QC, Canada, May 1999.
- [4] M. Buehler, R. Battaglia, A. Cocosco, G. Hawker, J. Sarkis, K. Yamazaki. Scout: A Simple quadruped that walks, climbs and runs. In *Proc. IEEE Int. Conf. Robotics and Automation*, pages 1707-1712, Leuven, Belgium, May 1998.
- [5] M. Buehler, A. Cocosco, K. Yamazaki, R. Battaglia. Stable Open Loop Walking in Quadruped Robots with Stick Legs. In *Proc. IEEE Int. Conf. Robotics and Automation*, pages 2348-2353, Detroit, Michigan, May 1999.
- [6] M. Bergerman, C. Lee, Y. Xu. Dynamic Coupling of Underactuated Manipulators. In *Proc. IEEE Conference on Control Application*, pages 500-505, Piscataway, New Jersey, 1995.
- [7] M. Bergerman, C. Lee, Y. Xu. Experimental Study of an Underactuated Manipulator. In *Proc. Int. Conf. on Intelligent Robots and Systems*, pages 693-707, Piscataway, New Jersey, 1995.
- [8] T. McGeer. Passive Walking with Knees. In *Proc. IEEE Int. Conf. Robotics and Automation*, pages 1640-1645, 1990.